

## Article

# Rapid and High-Performance Analysis of Total Nitrogen in Coco-Peat Substrate by Coupling Laser-Induced Breakdown Spectroscopy with Multi-Chemometrics

Bing Lu <sup>1</sup>, Xufeng Wang <sup>2</sup>, Can Hu <sup>2</sup>  and Xiangyou Li <sup>1,\*</sup> 

<sup>1</sup> Wuhan National Laboratory for Optoelectronics (WNLO), Huazhong University of Science and Technology (HUST), Wuhan 430074, China; 2021509011@hust.edu.cn

<sup>2</sup> College of Mechanical and Electrical Engineering, Tarim University, Alar 843300, China; wxf@taru.edu.cn (X.W.); 120140004@taru.edu.cn (C.H.)

\* Correspondence: xyli@mail.hust.edu.cn

**Abstract:** Nitrogen is an important nutrient element for crop growth. Rapid and accurate acquisition of nitrogen content in cultivation substrate is the key to precise fertilization. In this study, laser-induced breakdown spectroscopy (LIBS) was used to detect the total nitrogen (TN) of coco-peat substrate. A LIBS spectrum acquisition system was established to collect the spectral line signal of samples with wavelengths ranging from 200 nm to 860 nm. Synergy interval partial least squares (Si-PLS) algorithm and elimination of uninformative variables (UVE) algorithm were used to select the spectral data of TN characteristic lines in coco-peat substrate. Univariate calibration curve and partial least squares regression (PLSR) were used to build mathematical models for the relationship between the spectral data of univariate characteristic spectral lines, full variables and screened multi-variable characteristic spectral lines of samples and reference measurement values of TN. By comparing the detection performance of calibration curves and multivariate spectral prediction models, it was concluded that UVE was used to simplify the number of spectral input variables for the model and PLSR was applied to construct the simplest multivariate model for the measurement of TN in the substrate samples. The model provided the best measurement performance, with the calibration set determination coefficient ( $R_c^2$ ) and calibration set root mean square error (RMSEC) values of 0.9944 and 0.0382%, respectively; the prediction set determination coefficient ( $R_p^2$ ) and prediction set root mean square error (RMSEP) had values of 0.9902 and 0.0513%, respectively. These results indicated that the combination of UVE and PLSR could make full use of the variable information related to TN detection in the LIBS spectrum and realize the rapid and high-performance measurement of TN in coco-peat substrate. It would provide a reference for the rapid and quantitative assessment of nutrient elements in other substrate and soil.

**Keywords:** coco-peat substrate; total nitrogen; laser-induced breakdown spectroscopy; synergy interval partial least squares; uninformative variables elimination



**Citation:** Lu, B.; Wang, X.; Hu, C.; Li, X. Rapid and High-Performance Analysis of Total Nitrogen in Coco-Peat Substrate by Coupling Laser-Induced Breakdown Spectroscopy with Multi-Chemometrics. *Agriculture* **2024**, *14*, 946. <https://doi.org/10.3390/agriculture14060946>

Academic Editor: Matteo Perini

Received: 7 May 2024

Revised: 11 June 2024

Accepted: 15 June 2024

Published: 17 June 2024



**Copyright:** © 2024 by the authors. Licensee MDPI, Basel, Switzerland. This article is an open access article distributed under the terms and conditions of the Creative Commons Attribution (CC BY) license (<https://creativecommons.org/licenses/by/4.0/>).

## 1. Introduction

Substrate culture is a soilless culture technology that uses solid media instead of soil to fix plant roots and provide nutrients through the substrate [1]. This technology can achieve high-quality and high-yield planting through the scientific management of water and fertilizer and precise environmental regulation [2]. Substrate cultivation can realize three-dimensional planting, which has the advantages of saving water, fertilizer and space, and has developed rapidly in urban agriculture in China in recent years [3]. Coco-peat substrate, as a renewable cultivation matrix formed by coconut shell processing, has many advantages [4,5]. It is widely used in soilless cultivation of fruits, vegetables and flowers in China. The precise control of water and fertilizer is crucial for substrate culture [6]. The

acquisition of substrate nutrients and water information is an important prerequisite for accurate management of water and fertilizer.

The nutrient requirement of nitrogen is very large during crop growth. Nitrogen is also the main component of protein, closely related to crop stem and leaf growth and fruit development, and is also an important nutrient element that directly affects crop yield and quality [7,8]. Total nitrogen (TN) is an important indicator to comprehensively reflect the nitrogen level in the growing environment. The application of nitrogen-containing chemical fertilizers can increase the soil/substrate nitrogen level [9]. Because it is difficult to rapidly and accurately grasp the TN content of the sample, it is impossible to evaluate the TN level of coco-peat substrate quickly. At present, the application of nitrogen fertilizer is often based on planting experience, which makes it difficult to achieve an accurate control of nitrogen fertilizer, resulting in excessive or insufficient application of nitrogen fertilizer. Excessive use of nitrogen fertilizer not only causes a large amount of waste of chemical fertilizer, but also easily produces serious environmental pollution [10]. Insufficient application of nitrogen fertilizer will lead to the failure to achieve the expected yield target and will affect the growth quality of crops.

To realize the precise management of nutrient elements in the process of planting, a soil testing formula is often used to guide scientific fertilization in practice. At present, the soil formulation is mainly determined by the traditional chemical analysis method to test the reference values of various nutrient elements in soil. This method cannot achieve the mass detection of samples and has poor real-time detection performance, which makes it difficult to quickly obtain large-scale farmland soil formulation data [11,12]. Due to the limitations of traditional methods, they cannot meet the real-time requirements of production management in modern facility agriculture. In addition, traditional chemical analysis methods require the generation of complex chemical reactions, which has some disadvantages such as strong operation professionalism, a time-consuming testing process and unfriendly environment [13]. Therefore, the rapid assessment of TN level in coco-peat substrate by advanced photoelectric detection technology is conducive to achieving accurate nitrogen control in soilless cultivation in facility agriculture, improving crop yield and quality, and protecting the environment.

Laser-induced breakdown spectroscopy (LIBS) is a widely used spectral analysis technique for the detection of atoms, ions and molecules [14]. It uses a focusing mirror to focus a pulse laser on the surface layer of the sample; the focused large-energy density laser ablates the sample to form plasma, and then a spectrometer is applied to analyze the collected plasma spectral signals [15]. The LIBS detection model of the component to be measured was established by constructing the mathematical relationship between the plasma spectral signals of the correction set samples and the reference value of the concentration of the component to be measured. The sample concentration information of the component to be measured could be obtained quickly by substituting the LIBS spectral data of the sample to be measured into the established LIBS detection model. LIBS was widely applied in the field of agriculture due to its advantages of simple sample preparation, fast detection speed, remote detection, in situ detection and multi-element simultaneous detection [16]. Xu et al. [17] realized the rapid identification of citrus huanglongbing (HLB) by combining LIBS with near-infrared spectroscopy. Lin et al. [18] used deep learning to assist LIBS in identifying the geographical origin of crops so as to achieve food traceability. Sun et al. [19] used LIBS combined with a machine learning algorithm to identify the original source of *Angelica dahurica* medicinal herbs. Borduchi et al. [20] used calibration-free LIBS and one-point calibration to quantitatively detect Ga, Mg and Fe content in soybean leaf. Zhang et al. [21] measured the magnesium content in citrus leaves by LIBS to achieve an indirect measurement of soluble solid content. Li et al. [22] realized rapid identification of seed varieties by combining LIBS with convolutional neural network. At present, many works have also been carried out using LIBS in the rapid detection of soil elements, but there is little research on the detection of cultivation substrate components. For example, Tavares et al. [23] used a spectral variable screening algorithm to screen

the LIBS characteristics of soil nutrients, and then constructed soil nutrient prediction models by comparing the performance of different modeling algorithms so as to obtain the best model for soil nutrient LIBS detection; Hossen et al. [24] used a combination of unmanned aerial vehicles multispectral imaging, LIBS, and artificial intelligence to achieve a rapid and efficient assessment of soil TN; Khoso et al. [25] used calibration-free LIBS to rapidly detect heavy metals in soils planted with different crops; Erler et al. [26] applied a portable LIBS detection device and the constructed multiple regression model to rapidly detect multiple nutrient elements in soil; and Ding et al. [27] enhanced the detection accuracy of heavy metals in oily soil through the combination of interval partial least squares and LIBS. In summary, LIBS had good feasibility in the rapid detection of agricultural substrate elements, and it would provide data support for the decision-making of precision agriculture fertilization. However, the matrix effect caused by complex matrix composition and the interference caused by atmospheric nitrogen on the TN content detection of samples had become a big challenge for the rapid and stable LIBS detection of coco-peat substrate TN content. The stability of a conventional univariate calibration curve in the actual detection of soil nutrient elements by LIBS was poor. A multivariate model could effectively overcome the influence of the matrix effect and significantly improve the measurement performance and stability of LIBS [28]. Vacuum environment measurement and injection gas isolation measurement were effective ways to solve the influence of atmospheric nitrogen on the LIBS detection of sample nitrogen elements. Compared with the vacuum environment measurement needed to provide complex equipment assistance, the inert gas isolation measurement had more advantages.

The selection of spectral line variables was very important for the establishment of a stable and reliable multivariate model [29]. Conventional univariate calibration curves usually selected the univariate strong spectral line characteristics of the elements to be measured based on the National Institute of Standards and Technology (NIST) database. This univariate model was greatly influenced by spectral line interference and matrix difference, and its detection accuracy and robustness were poor [30]. The multivariate discrete spectral line features and continuous spectral line feature sub-intervals of the element to be measured could be selected by a statistical method so as to obtain the comprehensive spectral signal of the detected element [31]. Then, the spectral information of multi-spectral line variables was fully utilized by multivariate modeling method to enhance the measurement performance of the spectral model. Moreover, the composition of coco-peat substrate was obviously disparate from that of soil, and the existing LIBS detection model of soil elements could not be applied for rapid analysis of the substrate elements. According to the relevant literature, the influence of the matrix effect on spectral detection could also be effectively eliminated by multivariate selection combined with a multivariate model [32–34].

To solve the influence of the matrix effect and atmospheric nitrogen on the detection of TN in coco-peat substrate, argon injection, variable screening and multivariate modeling were combined to achieve rapid and high-performance detection of TN in coco-peat substrate, thus providing a basis for scientific fertilization decision-making. The specific works were as follows: (1) The optimal argon flow rate for the LIBS detection of TN content in coco-peat substrate was determined. (2) Spectral detection model of coco-peat substrate TN based on univariate calibration curve was established, and PLSR was used to construct the LIBS detection model of TN in coco-peat substrate based on full variable spectral data. (3) Synergy interval partial least squares (Si-PLS) and elimination of uninformative variables (UVE) were used to select the continuous and discrete characteristic variables, and the PLSR measurement model of TN in coco-peat substrate was established based on the selected variables. (4) An optimal LIBS model for the measurement of TN value of coco-peat substrate was determined by comparing the actual performance of the spectral models based on full variables, a single variable and screening multi-variables.

## 2. Materials and Methods

### 2.1. Preparation of Samples

Coco-peat substrate bricks manufactured by Galuku Pty Ltd. (Rose Bay, Australia) were selected for sample preparation in this experiment. Coco-peat substrate brick was quickly turned into a loose state by soaking in water, and the solid and liquid separation of sample and soaked water was achieved through screen filtration. Then, the substrate samples of various particle sizes were obtained by natural air-drying. To prepare experimental samples with various concentration gradients, different concentrations of urea (SCR, Sinopharm Chemical Reagent Co., Ltd., Ningbo, China) solution were added to the air-dried samples through simulated fertilization. After adding the nutrient solution, the samples were adsorbed for 24 h, and the samples were dried after adsorption so as to prepare experimental samples with different TN content. The prepared samples with different concentrations were crushed separately by using a pulverizer (Hangtai Multi-functional pulverizer, Hangtai Electronic Technology Co., Ltd., Hangzhou, China), and then the crushed samples were screened with a 0.5 mm mesh. Four high-concentration samples and eight low-concentration samples were prepared, respectively. The high- and low-concentration sample were selected from prepared samples, and the two samples were taken by electronic balance (FA-2004B, Shanghai Youke Instrument Co., Ltd., Shanghai, China) according to different mass ratios. Then, the weighed powder samples were placed in a 10 mL centrifuge tube for mixing, and the centrifuge tube was treated with a vortex mixer (NP-30S, Changzhou Empei Instrument Manufacturing Co., Ltd., Changzhou, China) for 6 min at maximum power to achieve uniform mixing of samples so as to prepare the substrate samples with various concentrations. Then, 1 g of mixed substrate sample and 9 g of boric acid (SCR, Sinopharm Chemical Reagent Co., Ltd., Ningbo, China) powder were weighed. Then, the compressed column samples were prepared by using an automatic tablet press (ZYP-40TS, Shanghai Xinnuo Instrument Equipment Co., Ltd., Shanghai, China) in the form of a boric acid inlay base. The sample preparation compression pressure and compression time of the automatic tablet press were set to 25 Mpa and 60 s, respectively [35]. A total of 84 cylindrical compressed samples with diameters of 40 mm and different TN contents were prepared.

### 2.2. Sample Spectral Data Acquisition

In this experiment, the spectral data of samples ranging from 200 nm to 860 nm were obtained by the self-built multi-functional LIBS spectrum acquisition system, and the structure of the system is shown in Figure 1. A Q-switched Nd: YAG laser (Quantel Brilliant B, Quantel, Newbury, UK); laser wavelength: 1064 nm; repetition frequency: 10 Hz; pulse duration: 5 ns) was chosen as the excitation light source of plasma. The laser produced a horizontal laser beam with a diameter of 9 mm, which was reflected by a dichroic mirror arranged at 45 degrees to be vertically transmitted, and the vertically transmitted laser beam was focused through a plano-convex mirror ( $f = 150$  mm) to ablate the sample. To avoid the plasma shielding effect caused by the laser breakdown of air, the laser focus was set 2 mm below the upper surface of the compressed sample by moving the displacement platform. Plasma emission signals generated by laser ablation of the coco-peat substrate were acquired by the collection head and coupled into the fiber. The collected spectral signals were transmitted to a spectrometer equipped with ICCD (iStar DH-334T, Oxford Instruments, Abingdon, UK) through an optical fiber. The inert gas argon was used for gas isolation to eliminate the interference of atmospheric nitrogen on the LIBS detection of TN content of coco-peat substrate. The protective gas was continuously supplied by compressed argon in the gas cylinder, and the flow rate of the supplied argon was accurately controlled by a gas flowmeter. In the process of signal acquisition, the collecting key parameters such as ablation laser energy, acquisition delay and acquisition gate width were set to 50 mJ, 1  $\mu$ s and 4  $\mu$ s, respectively. Each spectrum was obtained by accumulating 50 pulses, and each measurement was repeated five times.

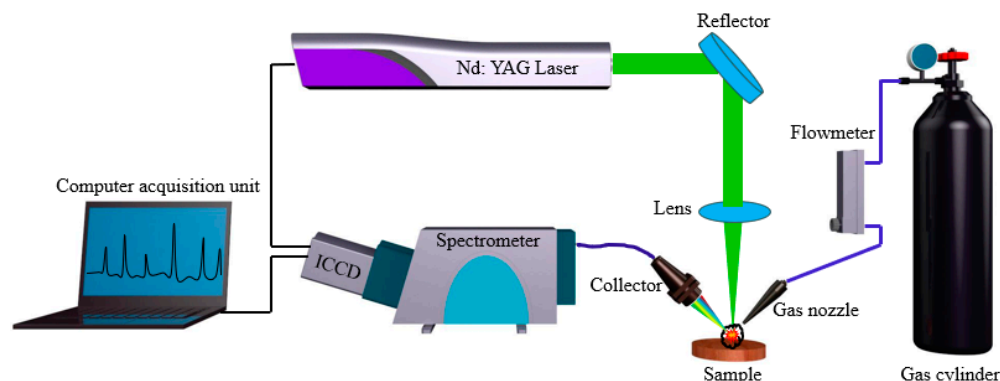


**Figure 1.** Diagram of LIBS spectrum detection system.

### 2.3. Determination of Sample TN Reference Value

The reference value of TN content in the substrate was determined by the China agricultural industry standard (NY/T 1121.24-2012) [36]. Some main steps of this method include the following: (1) samples were despoiled in a despoiling furnace; (2) an automatic nitrogen determinator was used to distill the boiled sample; (3) the nitrogen in the sample was converted into  $\text{NH}_3$  by distillation, and then the boric acid solution with acid-base indicator was used to absorb  $\text{NH}_3$ ; and (4) an acid standard solution was applied to titrate the boric acid solution that absorbed  $\text{NH}_3$ . TN values could be calculated by hydrochloric acid consumption, and the calculation formula is as shown in (1).

$$\omega = \frac{(V - V_0) \times C_H \times 0.014}{m(1 - f)} \times 100\% \quad (1)$$

where  $\omega$  is the TN content of sample (%);  $C_H$  is the actual concentration of HCl solution (mol/L);  $V$  is the amount of HCl solution consumed by the sample (mL);  $V_0$  is the amount of HCl solution consumed by the blank sample (mL); 0.014 is the molar mass of N (kg/mol);  $m$  is the mass of air-dried sample (g); and  $f$  is the moisture content of the substrate sample (%).

### 2.4. Selection of Spectral Features

LIBS data collected in this experiment contained spectral information of a variety of elements in the sample, and there were several spectral characteristic signals for the same element in the sample. A large number of variables unrelated to the elements to be tested would inevitably interfere with the detection accuracy to a certain extent when the TN modeling analysis was carried out applying the full variable spectral data. Although multi-variable modeling methods such as principal component analysis could reduce the interference of irrelevant variables by assigning different weight coefficients to each variable, these still increased the complexity of the model and affected the detection efficiency. Therefore, it was essential to select characteristic variables closely related to the analysis of the element to be detected for modeling analysis.

In LIBS detection, variables were often selected according to the characteristics of strong emission lines in NIST, and the calibration curve was established by using the selected univariate characteristics of elements to be detected. Due to the large variation in the actual sample matrix, the univariate calibration curve had problems such as poor anti-interference and unstable accuracy. To simplify the model and enhance the comprehensive measurement performance of the model, we proposed to construct a multivariate measurement model for a sample TN value by screening multivariate variables from the full variable spectrum. Therefore, Si-PLS and UVE were proposed to select continuous variable sub-intervals and discrete feature variables, respectively. The main idea of Si-PLS was to separate the full variable spectral data into several sub-intervals, establish a partial least squares model based on the continuous feature data of each sub-interval, and combine the corresponding sub-interval spectral data of several models with better prediction

performance by comparison so as to realize the selection of the optimal continuous feature variable sub-interval [37]. Si-PLS mainly included the following steps: (1) the partial least squares model of global variables was established; (2) the global variable was divided into 20 sub-intervals, and the regression models of spectral data in each sub-interval were established; (3) the results of steps (1) and (2) were compared, and the sub-interval with the best result was taken as the selection sub-interval; (4) the sub-interval selected in step (3) was taken as the central interval, and the variable region was expanded to both sides; and (5) four sub-intervals with better detection performance in the same partition were combined to complete the screening of synergy sub-intervals. UVE was a variable screening algorithm based on the analysis of a partial least squares regression coefficient, which mainly eliminated the variables that could not provide useful information [38]. The main principle of UVE was to combine the artificially generated noise matrix with the spectral matrix and TN reference value matrix to form a new matrix, through which the useless information threshold could be obtained, and then the useful information variables could be screened by comparing the stability of the regression coefficient with the decision threshold [39]. Some main steps of UVE were as follows: (1) a randomly generated noise matrix  $S$  and the spectral matrix  $X$  were combined to form the new matrix  $XR$ ; (2) the matrix  $XR$  and the concentration matrix  $Y$  were analyzed by partial least squares modeling, one sample was eliminated each time, and a number of partial least squares regression (PLSR) coefficients were obtained to form matrix  $B$ ; (3) the standard deviation  $s$  and the mean vector  $me$  of matrix  $B$  were calculated by column, and then the threshold  $h = me/s$  was calculated; and (4) irrelevant signals were removed according to the signal threshold  $h$ . The two variable selection algorithms were implemented in Matlab R2017 (Mathworks Inc., Natick, MA, USA).

### 2.5. Establishment and Evaluation of Model

Univariate calibration curve and PLSR were selected to construct the mathematical relationship between the spectral data of samples and the TN reference measurement value of the sample. The calibration curve was mainly to build the function relationship between univariate spectral data and physical and chemical reference values by linear and nonlinear fitting. PLSR was a statistical method that integrated the advantages of many typical regression algorithms. This algorithm spatially transformed the predictor and observed variables so that a line regression model was obtained [40]. PLSR was very suitable to handle multicollinearity between spectral data [41]. In this study, PLSR was applied to establish function models based on full variables, Si-PLS and UVE selected feature variables' data, and the calibration curve was used to construct the measurement model for univariate strong spectral line features screened based on NIST. PLSR is a classical multivariate modeling algorithm, and its modeling process is mainly completed by the relevant modeling modules in the Matlab toolbox. In the PLSR modeling process, the selection of the number of potential variables (LVs) was very important; too small a number of LVs would lead to poor model performance; and too large the number of LVs might lead to overfitting of the model. Therefore, the optimal number of LVs was determined by the minimizing predicted residual sum of squares, and the predicted residual sum of squares was calculated according to the method of leave-one-out cross-validation [42]. The model performance was mainly estimated by the determination coefficients ( $R^2$ ) and the root mean square errors (RMSE) [43].

## 3. Results and Discussion

### 3.1. Statistics of Reference Value of TN in Coco-Peat Substrate Samples

To build the function relationship between the LIBS data of the substrate samples and the TN reference measurement value of the samples, the TN measurement values of four high-concentration samples (the sample number was 9–12) and eight low-concentration samples (The sample number was 1–8) were determined by the method specified in the

China agricultural industry standard (NY/T 1121.24-2012) before preparing the mixed samples, and the measurement values are shown in Table 1.

**Table 1.** Measurement results of TN content in high- and low-concentration sample groups by China national standard method.

Sample Number	TN Content (%)						
1	0.394	4	0.333	7	0.354	10	1.494
2	0.410	5	0.382	8	0.324	11	1.990
3	0.361	6	0.345	9	0.964	12	2.404

In the process of mixing different concentration samples to prepare samples with various TN contents, the TN content of the prepared mixed samples could be calculated according to the mixing mass ratio of the two samples and the actual measured data in Table 1. According to the TN content of the prepared mixed samples, 84 samples were divided into two sets by the concentration gradient method at a ratio of 3:1. The distribution statistical characteristics of the reference measurement values of TN in the two sets of samples are shown in Table 2. The calibration dataset was used to train the spectral prediction model, and the other dataset was applied to test the performance of the measurement model.

**Table 2.** Statistics on distribution characteristics of TN reference measurement values in coco-peat substrate calibration set and prediction set samples.

Sample Set	Number of Samples	Range of TN Content (%)	Mean (%)	Standard Deviation (%)
Calibration set	63	0.333–2.404	1.042	0.519
Prediction set	21	0.361–2.197	1.028	0.516
Total samples	84	0.333–2.404	1.038	0.516

### 3.2. Analysis of Coco-Peat Substrate LIBS Spectral Characteristics

There is a large amount of nitrogen in the atmosphere, and atmospheric nitrogen will affect the LIBS detection of TN content in coco-peat substrate. To avoid atmospheric nitrogen contributing to the LIBS detection signal intensity of the substrate TN, atmospheric nitrogen was blocked from contacting with the laser ablated area by spraying argon gas. The flow rate of argon injection would directly affect the nitrogen isolation in the laser ablation area. Therefore, the influence of the argon injection flow rate on the TN content LIBS detection of coco-peat substrate was studied by collecting strong spectral line data of nitrogen element of the same substrate sample under different argon injection flow rates. Figure 2 shows the substrate LIBS spectral data of 742.36 nm, 744.23 nm and 746.83 nm at different argon injection flow rates.

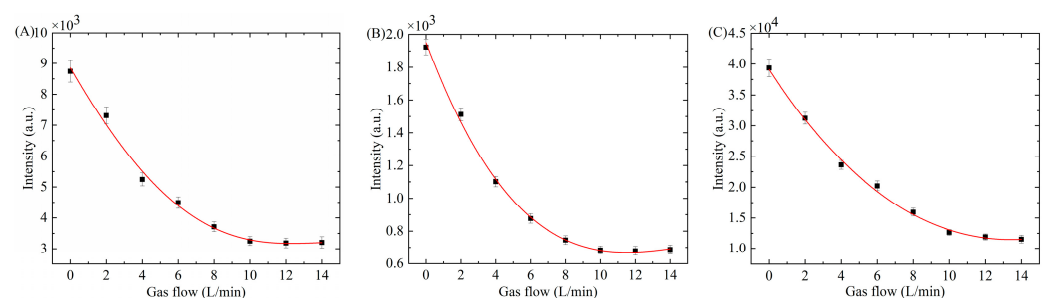


**Figure 2.** Influence of argon injection flow rate on the signal of TN. (A) 742.36 nm, (B) 744.23 nm, (C) 746.83 nm.

It can be seen from Figure 2 that the spectral line intensity of the LIBS spectrum was the highest when argon was not injected, which indicated that atmospheric nitrogen was also excited to produce nitrogen emission spectral line signals at the same time. With the increase in the argon injection flow rate, the emission signal of nitrogen element decreased sharply, which indicated that the nitrogen in the atmosphere was gradually isolated. The collected substrate LIBS signal intensity did not decrease when the argon injection flow rate was greater than or equal to 10 L/min. These results indicated that the atmosphere in the laser ablation area was isolated by argon; atmospheric nitrogen would not have a significant impact on the LIBS detection of TN content in the substrate. In addition, the fluctuation in LIBS spectral data was the largest when argon was not injected. With the gradual increase in the argon injection flow rate, the atmosphere in the laser ablation region was gradually isolated, and the collected LIBS signals gradually became stable. Therefore, the optimal argon injection flow rate for substrate TN content LIBS detection was determined to be 10 L/min based on reducing the amount of argon and avoiding the influence of excessive argon injection flow rate on plasma stability. Dib et al., also studied the effect of argon flow rate on CN molecule LIBS signal, and their conclusions were consistent with the optimal argon injection flow rate determined in this study [44]. The above results showed that atmospheric nitrogen had a significant impact on the TN detection of substrate samples, argon injection would effectively improve the signal quality of TN detection of samples, and the injection argon flow rate also had an impact on the signal quality of substrate TN detection. The interference of atmospheric nitrogen on substrate TN detection could be effectively eliminated by optimizing the parameter of injection argon flow rate.

According to the determined optimal LIBS detection parameters, the LIBS spectral data of all coco-peat substrate samples were collected. All the LIBS spectra had the same spectral line features, but there were some differences in the peak values of each spectral line feature. The above results showed that the substrate elements of each sample were similar, but the content of each element was different to some extent. Figure 3 is the original LIBS spectrum of a randomly selected substrate sample.

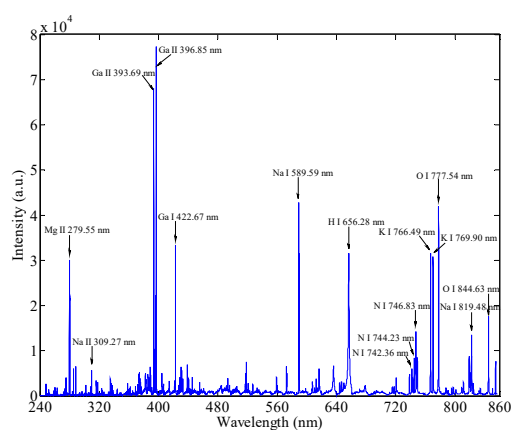


**Figure 3.** LIBS spectrum of coco-peat substrate.

It can be seen from Figure 3 that there were abundant nutrient elements in the substrate sample, and the spectral characteristic peaks of each nutrient element were significantly different. In addition, all samples had strong spectral line characteristics at wavelengths of 742.36 nm, 744.23 nm and 746.83 nm. Among the collected spectral signals of the substrate samples, there must be some spectral signals that were not related to the detection of TN content, which were interference signals for TN content LIBS detection. To eliminate the influence of background noise on LIBS detection, spectral data with a wavelength range of 722–737 nm were selected as the spectral background, and then the baseline correction was carried out by background deduction.

### 3.3. Calibration Curve Analysis of TN in Coco-Peat Substrate Based on Univariate LIBS Characteristics

To realize fast LIBS optical analysis of TN content in coco-peat substrate, the strong spectral lines feature data at sample wavelengths of 742.36 nm, 744.23 nm, and 746.83 nm were used as independent variables according to NIST, and the reference measurement values of TN obtained by the national standard method for each sample were used as dependent variables. Univariate fitting was applied to construct a mathematical relationship between the strong spectral lines feature data of the total samples and their TN reference measurement values, while the leave-one-out method was used for cross-validation. Table 3 shows the analysis results of the calibration curve of TN content based on the feature data of the abovementioned three strong spectral lines.

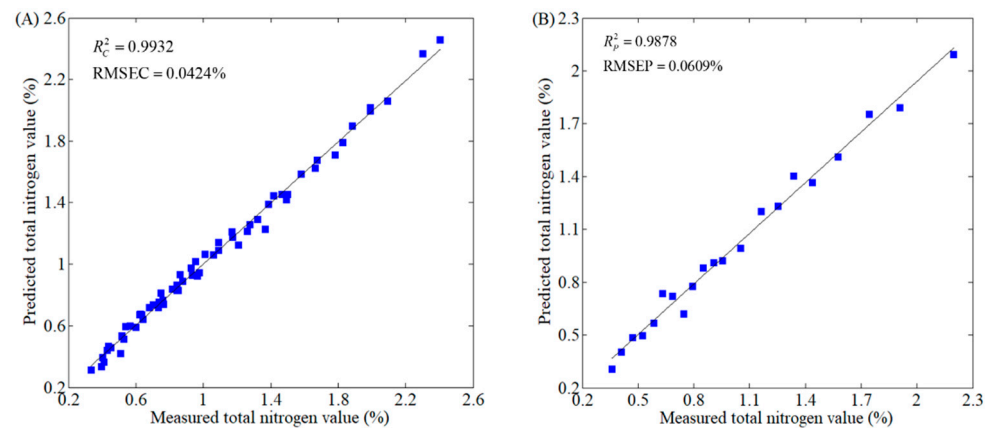
**Table 3.** Analysis results of TN calibration curves based on univariate LIBS spectral characteristics.

Characteristic Spectral Line	$R^2$	RMSECV
742.36 nm	0.0016	18.8751%
744.23 nm	0.0126	4.7245%
746.83 nm	0.0531	2.2082%

It can be seen from Table 3 that the determination coefficient of the univariate calibration curve of TN constructed by using the spectral data of the abovementioned three strong spectral line characteristic variables of nitrogen element was small, and the cross-validation root mean square error RMSECV of the model was large. These analysis results showed that the detection performance of the univariate prediction model using strong spectral line features was poor, and the measurement performance could not meet the actual detection requirements. Zhang et al., also confirmed this view in the study of LIBS detection of TN content in simulated Martian soil [45]. The univariate calibration curve based on strong spectral line features was the simplest modeling method in LIBS detection, but the variation in sample matrix composition would have a matrix effect on coco-peat substrate TN content detection, which would lead to poor anti-interference and low prediction accuracy of the univariate TN detection model. The useful information of the single variable to characterize the components to be measured was limited, and it was easily disturbed by the matrix. The single-variable calibration curve can only achieve better performance detection of the sample components under some ideal sample conditions. Therefore, the conventional calibration curve was not suitable for LIBS modeling analysis of coco-peat substrate TN content.

### 3.4. Detection of TN in Coco-Peat Substrate Based on Full Variables LIBS Data

In order to enhance the TN LIBS detection performance of coco-peat substrate, a multivariate input function model was applied to construct the mathematical model between the sample LIBS data and the reference values of TN. Firstly, the spectral matrix was formed by combining the full variable spectrum data of all the samples, and then the physicochemical matrix was formed by combining the TN reference values of all samples measured by the national standard method. PLSR was selected to build a multivariate mathematical model between spectral matrix and physicochemical matrix. Figure 4 shows the calibration set and predicted scatter plot of the coco-peat substrate TN spectral measurement model established based on the full variable LIBS data.



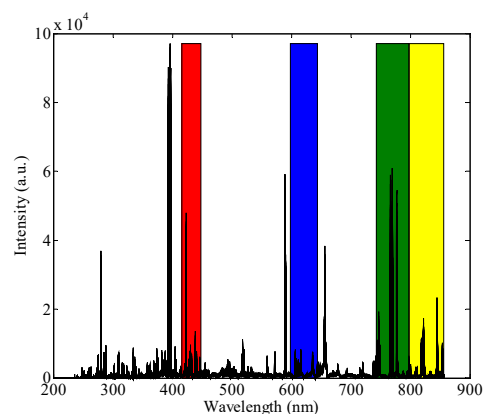
**Figure 4.** Scatter plot of PLSR model based on full variables LIBS spectrum. (A) Calibration set, (B) prediction set.

Figure 4 shows that the detection model of TN content of coco-peat substrate built by using full variable LIBS data had good performance;  $R_C^2$  and  $R_P^2$  had values of 0.9932 and 0.9878, respectively, and RMSEC and RMSEP had values of 0.0424% and 0.0609%, respectively. Compared with the results of univariate calibration curve analysis, the determination coefficient of the LIBS detection model established with the full variable LIBS spectral data was significantly improved, the root mean square error was sharply reduced, and the detection performance of the full variable model was comprehensively enhanced. The performance of the established multivariate detection model for the substrate TN content was similar to that reported in the literature for the determination of soil TN content under a vacuum or an argon environment [46,47]. The key to improve the anti-interference ability and accuracy of multivariate models was to increase the useful signals involved in modeling and the mutual constraints among variables. However, the input variable of the detection model was 23,614 when the full variable spectrum was selected to participate in the detection analysis, which made the detection model more complex and extended the detection time, thus affecting the detection efficiency. In summary, the full variable modeling could make maximum use of spectral information for analysis, but noise signals and some irrelevant interference signals would also be involved in modeling analysis, which inevitably presented greater challenges for multivariate modeling methods to identify useful information. At the same time, the complexity of the detection model was inevitably increased, which was not conducive to the development of special detection instruments.

### 3.5. Detection of TN Content in Coco-Peat Substrate Based on LIBS Data of Screening Characteristic Variables

#### 3.5.1. Modeling of Characteristic Variables for Si-PLS Screening

The obtained coco-peat substrate LIBS spectral data were separated into 20 consecutive sub-intervals by Si-PLS, and the prediction model was constructed by randomly selecting the spectral data corresponding to several sub-intervals from the divided sub-intervals, and the assessment indicator of root mean square error was applied to select the best synergy sub-intervals. The Si-PLS model with the best detection performance was obtained by comparison, and the corresponding sub-intervals were the optimal interval combination. Figure 5 shows the optimal interval combination selected by Si-PLS. The model of the optimal interval combination spectral data was used to detect the TN content of the samples, and the detection performance is presented in Figure 6.



**Figure 5.** The optimal interval combination of sample TN features selected by Si-PLS.

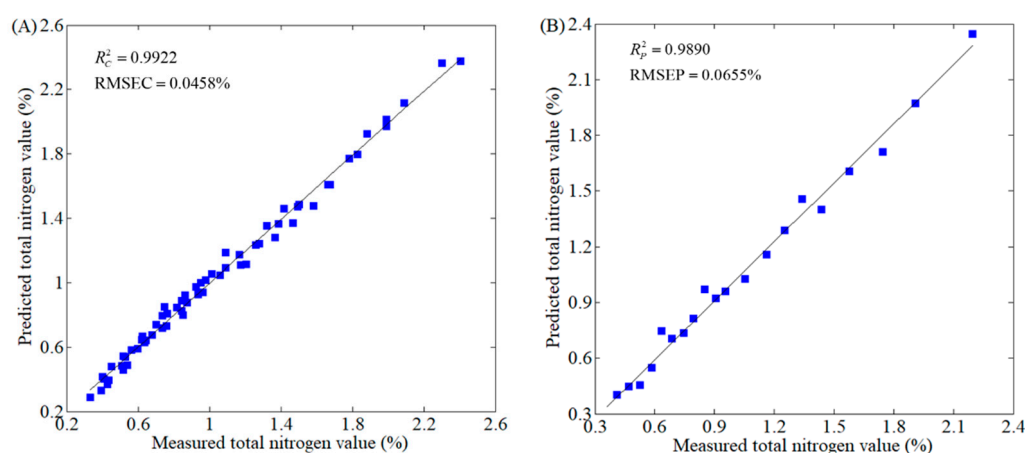


**Figure 6.** Scatter diagram of PLSR prediction model for screening spectral variables by Si-PLS. (A) Calibration set, (B) prediction set.

As can be seen from Figure 5, Si-PLS was applied to select the continuous feature variable sub-intervals, and four optimal synergy sub-intervals were obtained by comparison, which effectively eliminated the spectral data of 16 sub-intervals with little correlation with the TN content detection. The number of variables that actually participated in the measurement was reduced from 23,614 to 4720, thus greatly simplifying the complexity of the model. Meanwhile, the four continuous characteristic variable intervals screened by Si-PLS were 416–448 nm, 599–644 nm, 743–798 nm and 798–857 nm, respectively. The selected optimal synergy subintervals included LIBS spectral data, such as 744.23 nm and 746.83 nm, which reflected the characteristics of strong spectral lines of nitrogen. The results of Dong et al., showed that the spectral data at the wavelengths of 744.23 nm and 746.83 nm had a great contribution to the LIBS detection of TN content [46]. As shown in Figure 6, the PLSR model constructed by Si-PLS screening four optimal synergy sub-intervals spectral data had a good prediction performance, with an  $R_c^2$  and RMSEC of 0.9922 and 0.0458%, and an  $R_p^2$  and RMSEP of 0.9890 and 0.0655%, respectively. Compared with the PLSR model of TN established by full variable spectral data, the detection accuracy was slightly affected, but the model was greatly simplified. The optimal interval combination selected by Si-PLS included some spectral line characteristics reflecting the variation in nitrogen elements, which was the key to construct the TN measurement model of coco-peat substrate with good detection performance. Since the selection of characteristic spectral lines by Si-PLS was directly related to the interval combination, some relevant information variables with low contribution were discarded; so, the detection performance of Si-PLS screening variable model was slightly worse than that of the full variable data model.

### 3.5.2. Modeling of Spectral Features for UVE Screening

The full variable LIBS data of coco-peat substrate contained rich element information of the constituent samples, and there were some signals that were not relevant to the detection of TN content. Irrelevant information participation in modeling not only interfered with the LIBS measurement of the substrate TN content, but also seriously affected the analysis and detection efficiency of the model. Therefore, UVE was applied to remove redundant and irrelevant signal variables from the acquired full variable LIBS data and screen information variables related to the test of coco-peat substrate TN content. The screening results of variables are shown in Figure 7.

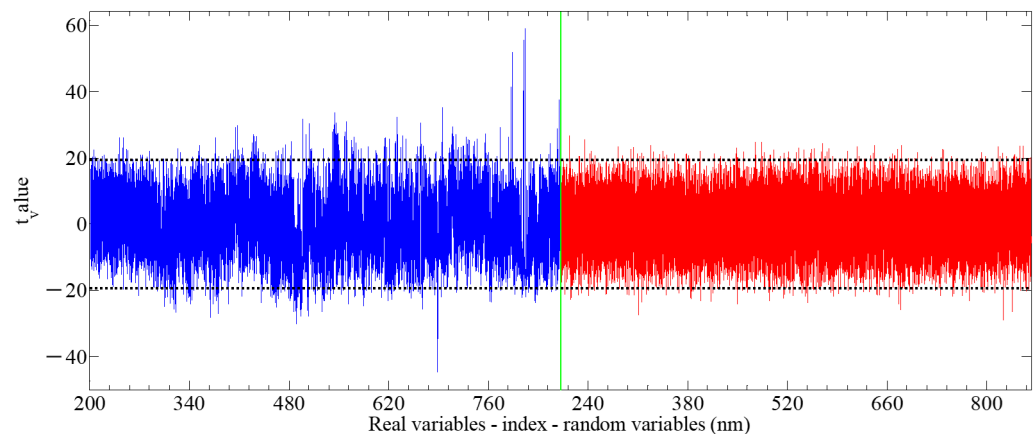


**Figure 7.** LIBS spectral characteristic lines of coco-peat substrate TN screened by UVE.

As can be seen from Figure 7, the abscissa and ordinate represent the wavelength and the stability of wavelength variables, respectively. The left side of the graph is the LIBS signal, the right side of the graph is the artificially added noise signal, and the two black horizontal dashed lines represent the boundaries of useful information or noise signals. The corresponding spectral variables are the UVE screening characteristic spectral lines when the stability of the left spectral variables exceeded the decision boundaries of two black dashed line. And the wavelength variable with signal stability within two black horizontal dashed lines is the irrelevant information variable of coco-peat substrate TN detection. Finally, PLSR was applied to construct the LIBS detection model of TN content based on UVE removing redundant signals, and its prediction performance is shown in Figure 8.

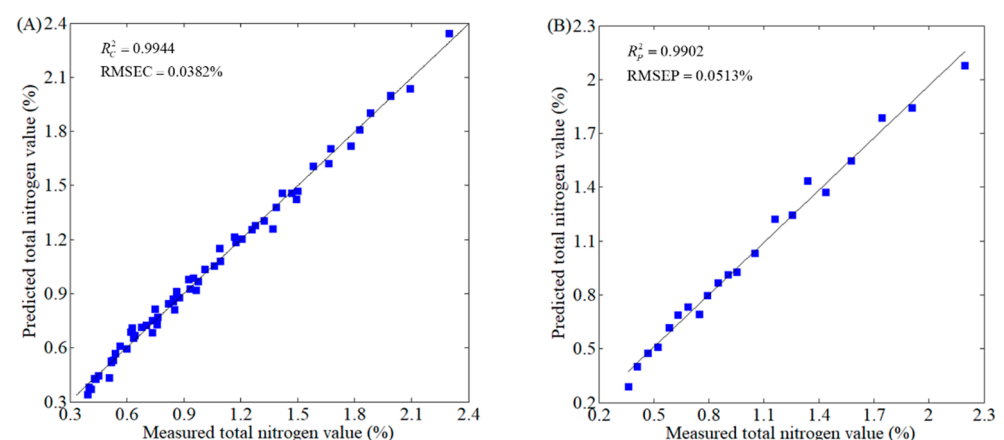


**Figure 8.** Scatter diagram of PLSR prediction model for screening spectral variables by UVE. (A) Calibration set, (B) prediction set.

It can also be seen from Figure 7 that the characteristic variables of the substrate TN detection decreased from 23,614 to 796 when UVE was applied to select LIBS feature lines. Many irrelevant information variables in the full variable data of the sample were eliminated, and the input variables of the measurement model were greatly reduced. In addition, UVE selected spectral lines data with a wavelength of 388.3 nm and nearby for modeling. Further analysis showed that CN molecular emission line signals with a wavelength of 388.3 nm had a good correlation with TN content detection in the substrate [48]. Therefore, this was also the reason why the UVE screening variable establishment model had the best performance. The prediction accuracy of PLSR detection model based on UVE screening feature lines was excellent, with an  $R_C^2$  and RMSEC of 0.9944 and 0.0382%, and an  $R_P^2$  and RMSEP of 0.9902 and 0.0513%, respectively. Compared with the actual measurement results of the full variable PLSR model, the determination coefficient of the PLSR model built by UVE selecting characteristic data was increased and the root mean square error was reduced. In addition, the complexity of measurement model was greatly simplified, and its prediction performance was further improved. UVE could retain useful spectral signals and eliminate irrelevant information variables to the greatest extent, which not only ensured that the established multivariate model had better anti-interference ability, but also was the key reason for simplifying the model and ensuring prediction accuracy. In a word, UVE could effectively select the information variables related to detection and remove the irrelevant redundant information in the full spectrum data. Through the combination of UVE and PLSR, high-performance detection of TN content in coco-peat substrate could be achieved, and it was also conducive to the development of special detection instruments.

### 3.6. Performance Comparison of LIBS Detection Models for TN in Coco-Peat Substrate Based on Full Variables and Selected Characteristic Variables

In order to fully consider the accuracy of spectral detection and the detection efficiency of the model, the detection performance of the best prediction model of single-variable, full variables and selected characteristic variables LIBS data of coco-peat substrate was compared, and the results represented in Table 4. Through comparison, the simplest and optimal LIBS spectral model for TN detection in coco-peat substrate was obtained so as to achieve fast and high-precision measurement of coco-peat substrate TN content.

**Table 4.** Comparison of prediction performance of optimal models established by different variable selection methods.

Method of Variable Selection	Number of Variables	Number of Latent Variables (LVs)	Proportion of Participating Variables	$R^2$		RMSE	
				$R_C^2$	$R_P^2$	RMSEC	RMSEP
Univariate	1	/	0.004%	0.0531		2.2082%	
Full variables	23,614	10	100%	0.9932	0.9878	0.0424%	0.0609%
Si-PLS	4720	8	19.988%	0.9922	0.9890	0.0458%	0.0655%
UVE	796	9	3.371%	0.9944	0.9902	0.0382%	0.0513%

As shown in Table 4, it was difficult to achieve a fast measurement of sample TN content with the univariate spectral calibration curve based on strong spectral line characteristics of nitrogen elements. The calibration set and prediction set model evaluation indexes ( $R^2$  and RMSE) of PLSR models established with full variables, Si-PLS and UVE screening variables were similar, which indicated that there was no overfitting phenomenon in the prediction models established with the optimal number of LVs. The PLSR model established by the full variable spectral data could realize a good detection performance of TN. The spectral prediction model established by UVE and Si-PLS selecting feature data could also realize the fast measurement of coco-peat substrate TN content. These variables involved in Si-PLS screening accounted for 19.988% of the total variables, and the variables selected by UVE accounted for only 3.371% of the total variables. The above results indicated that the two variable selection algorithms (UVE and Si-PLS) could efficiently extract the spectral information related to the measurement of TN in the full variable spectral data,

and significantly reduce the redundant data in the model input variables. Further analysis showed that the matrix effect was the main reason for the difficulty in realizing LIBS detection of substrate TN content in the univariate calibration curve, and multi-variable analysis modeling would effectively solve the problems caused by the matrix effect [23]. In addition, the atomic emission lines and CN molecular emission lines related to the detection of TN in coco-peat substrate could be fully screened through the combination of variable screening and multivariate modeling, which was conducive to the mining of LIBS spectral information and the realization of high-performance detection. The contradiction between the insufficient spectral information of the univariate calibration curve and the excessive and redundant information of the full spectrum modeling could be solved by variable optimization and multivariate modeling. Compared with the full variable optimal spectral prediction model, the PLSR model established by UVE screening variables not only simplified the complexity of the model to the greatest extent, but also further enhanced the detection performance. The full utilization of LIBS spectral information might be the main reason why UVE combined with PLSR achieved high-performance detection of TN content in coco-peat substrate. In summary, UVE was applied to select the feature variable data, and the best TN measurement model would be constructed by PLSR, with an  $R_C^2$  and RMSEC of 0.9944 and 0.0382%, and an  $R_p^2$  and RMSEP of 0.9902 and 0.0513%, respectively. Compared with the existing literature on soil total nitrogen LIBS detection, the combination of UVE and PLSR could achieve excellent performance detection of the substrate TN content.

#### 4. Conclusions

In this study, LIBS was used to achieve rapid and high-performance detection of TN content in coco-peat substrate. The multivariate model could effectively reduce the influence of matrix effect, which was more conducive to establishing a better coco-peat substrate TN detection model than the univariate calibration curve. UVE and Si-PLS could effectively extract the closely related spectral signals of the substrate LIBS detection. At the same time, variable screening and multivariate modeling could make full use of the atomic emission lines and CN molecular emission lines information related to TN detection in the LIBS spectrum of coco-peat substrate. Through comparison, the optimal and simplest high-performance model for TN content detection of coco-peat substrate would be established by combining UVE and PLSR. The  $R_C^2$  and RMSEC of the optimal model were 0.9944 and 0.0382%, and the  $R_p^2$  and RMSEP were 0.9902 and 0.0513%, respectively. In summary, UVE combined with PLSR was beneficial to the development of special LIBS detection instrument for TN content in coco-peat substrate. At present, there are few studies on the rapid detection of elements in facility cultivation substrate by LIBS. This study is of great significance to promote the substrate cultivation of facility agriculture to achieve precision fertilization. In the future, the robustness and universality of the model would be further improved by increasing the type and number of training model samples.

**Author Contributions:** Writing—review and editing, B.L.; conceptualization and methodology, X.W.; resources and data curation, C.H.; supervision, X.L. All authors have read and agreed to the published version of the manuscript.

**Funding:** This work was supported by the National Natural Science Foundation of China (32301694, 62305123).

**Institutional Review Board Statement:** Not applicable.

**Informed Consent Statement:** Not applicable.

**Data Availability Statement:** The data presented in this study are available on request from the corresponding author.

**Acknowledgments:** The authors are grateful to the anonymous reviewers for their comments.

**Conflicts of Interest:** The authors declare no conflicts of interest.

## References

- Chen, C.; Zhang, X.L.; Xu, K.; Su, X.Q.; Sun, J. Compensation methods for pH direct measurement in soilless culture substrates using the all-solid-stated pH sensor. *IEEE Sens. J.* **2021**, *21*, 26856–26867. [[CrossRef](#)]
- Khater, E.S.; Bahnasawy, A.; Abass, W.; Morsy, O.; El-Ghobashy, H.; Shaban, Y.; Egela, M. Production of basil (*Ocimum basilicum* L.) under different soilless cultures. *Sci. Rep.* **2021**, *11*, 12754. [[CrossRef](#)] [[PubMed](#)]
- Fussy, A.; Papenbrock, J. An overview of soil and soilless cultivation techniques-chances, challenges and the neglected question of sustainability. *Plants* **2022**, *11*, 1153. [[CrossRef](#)]
- Ghoreishy, F.; Ghehsareh, A.M.; Fallahzade, J. Using composted wheat residue as a growth medium in culture of tomato. *J. Plant Nutr.* **2018**, *41*, 766–773. [[CrossRef](#)]
- Li, B.; Gu, S.; Chu, Q.; Yang, Y.L.; Xie, Z.J.; Fan, K.J.; Liu, X.G. Development of transplanting manipulator for hydroponic leafy vegetables. *Int. J. Agric. Biol. Eng.* **2019**, *12*, 38–44. [[CrossRef](#)]
- Ahmad, U.; Alvino, A.; Marino, S. Solar fertigation: A sustainable and smart IoT-based irrigation and fertilization system for efficient water and nutrient management. *Agronomy* **2022**, *12*, 1012. [[CrossRef](#)]
- Ferrón-Carrillo, F.; Cunha-Chiamolera, T.P.L.; Urrestarazu, M. Effect of ammonium nitrogen on pepper grown under soilless culture. *J. Plant Nutr.* **2021**, *45*, 113–122. [[CrossRef](#)]
- Kim, M.J.; Lee, J.E.; Back, I.; Lim, K.J.; Mo, C. Estimation of total nitrogen content in topsoil based on machine and deep learning using hyperspectral imaging. *Agriculture* **2023**, *13*, 1975. [[CrossRef](#)]
- Wang, Y.T.; Li, M.Z.; Ji, R.H.; Wang, M.J.; Zhang, Y.; Zheng, L.H. Construction of complex features for predicting soil total nitrogen content based on convolution operations. *Soil Tillage Res.* **2021**, *213*, 105109. [[CrossRef](#)]
- Zhao, P.F.; Xing, J.F.; Hu, C.; Guo, W.S.; Wang, L.; He, X.W.; Xu, Z.X.; Wang, X.F. Feasibility of near-infrared spectroscopy for rapid detection of available nitrogen in vermiculite substrates in desert facility agriculture. *Agriculture* **2022**, *12*, 411. [[CrossRef](#)]
- Recena, R.; Fernández-Cabanás, V.M.; Delgado, A. Soil fertility assessment by Vis-NIR spectroscopy: Predicting soil functioning rather than availability indices. *Geoderma* **2019**, *337*, 368–374. [[CrossRef](#)]
- Coutinho, M.A.N.; Alari, F.O.; Ferreira, M.M.C.; do Amaral, L.R. Influence of soil sample preparation on the quantification of NPK content via spectroscopy. *Geoderma* **2019**, *338*, 401–409. [[CrossRef](#)]
- Zhang, B.H.; Sha, W.; Jiang, Y.C.; Cui, Z.F. Quantitative analysis of nitrogen in ammonium phosphate fertilizers using laser-induced breakdown spectroscopy. *Appl. Optics* **2019**, *58*, 3277–3281. [[CrossRef](#)]
- Zhong, J.; Jiang, X.M.; Lin, M.; Dai, H.L.; Zhu, F.L.; Qiao, X.; Zhao, Z.F.; Peng, J.Y. Fast quantification of matcha adulterants with laser-induced breakdown spectroscopy spectrum and image. *Comput. Electron. Agric.* **2023**, *209*, 107813. [[CrossRef](#)]
- Xu, X.B.; Du, C.W.; Ma, F.; Shen, Y.Z.; Wu, K.; Liang, D.; Zhang, J.M. Detection of soil organic matter from laser-induced breakdown spectroscopy (LIBS) and mid-infrared spectroscopy (FTIR-ATR) coupled with multivariate techniques. *Geoderma* **2019**, *355*, 113905. [[CrossRef](#)]
- Lin, Z.J.; Zhang, N.; Xu, Z.Y.; Liao, J.P.; Yuan, H.; Chenshen, E.F.; Liu, J.M.; Li, J.M.; Zhao, N.; Zhang, Q.M. Modified iterative wavelets for background removal in laser-induced breakdown spectroscopy based on fiber laser ablation. *J. Anal. At. Spectrom.* **2022**, *37*, 2082–2088. [[CrossRef](#)]
- Xu, F.H.; Hao, Z.Q.; Huang, L.; Liu, M.H.; Chen, T.B.; Chen, J.Y.; Zhang, L.Y.; Zhou, H.M.; Yao, M.Y. Comparative identification of citrus huanglongbing by analyzing leaves using laser-induced breakdown spectroscopy and near-infrared spectroscopy. *Appl. Phys. B-Lasers Opt.* **2020**, *126*, 43. [[CrossRef](#)]
- Lin, P.; Wen, X.L.; Ma, S.X.; Liu, X.C.; Xiao, R.H.; Gu, Y.F.; Chen, G.H.; Han, Y.X.; Dong, D.M. Rapid identification of the geographical origins of crops using laser-induced breakdown spectroscopy combined with transfer learning. *Spectrosc. Acta Pt. B-Atom. Spectr.* **2023**, *206*, 106729. [[CrossRef](#)]
- Sun, J.X.; Li, H.L.; Yao, Y.H.; Yan, Q.Y.; Dong, F. Angelica dahurica using LIBS technology combined with machine learning algorithms. *Optoelectron. Lett.* **2024**, *20*, 171–176. [[CrossRef](#)]
- Borduchi, L.C.L.; Milori, D.M.B.P.; Meyer, M.C.; Villas-Boas, P.R. Reducing matrix effects on the quantification of Ca, Mg, and Fe in soybean leaf samples using calibration-free LIBS and one-point calibration. *Spectrosc. Acta Pt. B-Atom. Spectr.* **2022**, *198*, 106561. [[CrossRef](#)]
- Zhang, D.; Zhao, Z.F.; Zhang, S.Y.; Chen, F.; Sheng, Z.Q.; Deng, F.; Zeng, Q.D.; Guo, L.B. Accurate identification of soluble solid content in citrus by indirect laser-induced breakdown spectroscopy with its leaves. *Microchem. J.* **2021**, *169*, 106530. [[CrossRef](#)]
- Li, X.L.; He, Z.N.; Liu, F.; Chen, R.Q. Fast identification of soybean seed varieties using laser-induced breakdown spectroscopy combined with convolutional neural network. *Front. Plant Sci.* **2021**, *12*, 714557. [[CrossRef](#)] [[PubMed](#)]
- Tavares, T.R.; Mouazen, A.M.; Nunes, L.C.; dos Santos, F.R.; Melquiades, F.L.; da Silva, T.R.; Krug, F.J.; Molin, J.P. Laser-Induced Breakdown Spectroscopy (LIBS) for tropical soil fertility analysis. *Soil Tillage Res.* **2022**, *216*, 105250. [[CrossRef](#)]
- Hossen, M.A.; Diwakar, P.K.; Ragi, S. Total nitrogen estimation in agricultural soils via aerial multispectral imaging and LIBS. *Sci. Rep.* **2021**, *11*, 12693. [[CrossRef](#)]
- Khoso, M.A.; Shaikh, N.M.; Kalhor, M.S.; Jamali, S.; Ujan, Z.A.; Raheel, A. Comparative elemental analysis of soil of wheat, corn, rice, and okra cropped field using CF-LIBS. *Optik* **2022**, *261*, 169247. [[CrossRef](#)]
- Erlor, A.; Riebe, D.; Beitz, T.; Löhmannsröben, H.G.; Gebbers, R. Soil nutrient detection for precision agriculture using handheld laser-induced breakdown spectroscopy (LIBS) and multivariate regression methods (PLSR, Lasso and GPR). *Sensors* **2020**, *20*, 418. [[CrossRef](#)] [[PubMed](#)]

27. Ding, Y.; Xia, G.Y.; Ji, H.W.; Xiong, X. Accurate quantitative determination of heavy metals in oily soil by laser induced breakdown spectroscopy (LIBS) combined with interval partial least squares (IPLS). *Anal. Methods* **2019**, *11*, 3657–3664. [[CrossRef](#)]
28. Sun, C.; Tian, Y.; Gao, L.; Niu, Y.S.; Zhang, T.L.; Li, H.; Zhang, Y.Q.; Yue, Z.Q.; Delepine-Gilon, N.; Yu, J. Machine learning allows calibration models to predict trace element concentration in soils with generalized LIBS spectra. *Sci. Rep.* **2019**, *9*, 11363. [[CrossRef](#)] [[PubMed](#)]
29. Zhang, Q.; Huang, W.Q.; Wang, Q.Y.; Wu, J.Z.; Li, J.B. Detection of pears with moldy core using online full-transmittance spectroscopy combined with supervised classifier comparison and variable optimization. *Comput. Electron. Agric.* **2022**, *200*, 107231. [[CrossRef](#)]
30. Yang, R.Z.; Bi, L.Q. Spectral enhancement mechanism and analysis of defocused collinear DP-LIBS technology. *Optik* **2021**, *243*, 167025. [[CrossRef](#)]
31. Zhu, A.F.; Xu, Y.; Ali, S.; Ouyang, Q.; Chen, Q.S. Au@Ag nanoflowers based SERS coupled chemometric algorithms for determination of organochlorine pesticides in milk. *LWT-Food Sci. Technol.* **2021**, *150*, 111978. [[CrossRef](#)]
32. Xu, W.J.; Sun, C.; Tan, Y.Q.; Gao, L.; Zhang, Y.Q.; Yue, Z.Q.; Shabbir, S.; Wu, M.T.; Zou, L.; Chen, F.Y.; et al. Total alkali silica classification of rocks with LIBS: Influences of the chemical and physical matrix effects. *J. Anal. At. Spectrom.* **2020**, *35*, 1641. [[CrossRef](#)]
33. Shabbir, S.; Xu, W.J.; Zhang, Y.Q.; Sun, C.; Yue, Z.Q.; Zou, L.; Chen, F.Y.; Yu, J. Machine learning and transfer learning for correction of the chemical and physical matrix effects in the determination of alkali and alkaline earth metals with LIBS in rocks. *Spectrosc. Acta Pt. B-Atom. Spectr.* **2022**, *194*, 106478. [[CrossRef](#)]
34. Chen, F.; Lu, W.J.; Chu, Y.W.; Zhang, D.; Guo, C.; Zhao, Z.F.; Zeng, Q.D.; Li, J.M.; Guo, L.B. High accuracy analysis of fiber-optic laser-induced breakdown spectroscopy by using multivariate regression analytical methods. *Spectrosc. Acta Pt. B-Atom. Spectr.* **2021**, *180*, 106160. [[CrossRef](#)]
35. Zhou, R.; Tang, Z.Y.; Liu, K.; Zhang, W.; Liu, K.; Li, X.Y.; Yang, P.; Li, G.Q. High sensitivity analysis of soil by laser-induced breakdown spectroscopy with Ag nanoparticles. *Opt. Laser Technol.* **2022**, *155*, 108386. [[CrossRef](#)]
36. NY/T 1121.24-2012; Soil Testing. Part 24: Determination of Total Nitrogen in Soil. Automatic Kjeldahl Apparatus Method. Farming Management Division, Ministry of Agriculture of the People's Republic of China: Beijing, China, 2012.
37. He, K.; Sun, Q.M.; Tang, X.Y. Prediction of tenderness of chicken by using viscoelasticity based on airflow and optical technique. *J. Texture Stud.* **2022**, *53*, 133–145. [[CrossRef](#)] [[PubMed](#)]
38. Hu, J.; Yang, L.; Lin, T.Z.; Shi, H.Y.; Qiao, P.; He, Y.; Liu, Y.D. Research on a LIBS-based detection method of medium-and-low alloy steel hardness. *J. Anal. At. Spectrom.* **2022**, *37*, 2309. [[CrossRef](#)]
39. Yang, L.; Meng, L.W.; Gao, H.Q.; Wang, J.Y.; Zhao, C.; Guo, M.M.; He, Y.; Huang, L.X. Building a stable and accurate model for heavy metal detection in mulberry leaves based on a proposed analysis framework and laser-induced breakdown spectroscopy. *Food Chem.* **2021**, *338*, 127886. [[CrossRef](#)]
40. Pornchaloempong, P.; Sharma, S.; Phanomsophon, T.; Srisawat, K.; Inta, W.; Sirisomboon, P.; Prinyawiwatkul, W.; Nakawajana, N.; Lapcharoensuk, R.; Teerachaichayut, S. Non-destructive quality evaluation of tropical fruit (mango and mangosteen) purée using near-infrared spectroscopy combined with partial least squares regression. *Agriculture* **2022**, *12*, 2060. [[CrossRef](#)]
41. Mishra, P.; Xu, J.L.; Liland, K.H.; Tran, T. META-PLS modelling: An integrated approach to automatic model optimization for near-infrared spectra. *Anal. Chim. Acta* **2022**, *122*, 340142. [[CrossRef](#)]
42. Qiao, L.; Tang, X.Y.; Dong, J. A feasibility quantification study of total volatile basic nitrogen (TVB-N) content in duck meat for freshness evaluation. *Food Chem.* **2017**, *237*, 1179–1185. [[CrossRef](#)] [[PubMed](#)]
43. Cheng, P.; Yin, L.M.; El-Seedi, H.R.; Zou, X.B.; Guo, Z.M. Green reduction of silver nanoparticles for cadmium detection in food using surface-enhanced Raman spectroscopy coupled multivariate calibration. *Food Chem.* **2022**, *394*, 133481. [[CrossRef](#)]
44. Dib, S.R.; Nespeca, M.G.; Junior, A.S.; Ribeiro, C.A.; Crespi, M.S.; Neto, J.A.G.; Ferreira, E.C. CN diatomic emission for N determination by LIBS. *Microchem. J.* **2020**, *157*, 105107. [[CrossRef](#)]
45. Zhang, B.Y.; Sun, C.; Yu, X.W.; Chen, F.Y.; Wang, L.; Rao, Y.F.; Sun, T.Y.; Zhao, Y.Y.S.; Yu, J. Sensitive and accurate determination of nitrogen in simulated Martian soil and environment with LIBS spectrum fusion and regression based on neural network. *Spectrosc. Acta Pt. B-Atom. Spectr.* **2023**, *206*, 106708. [[CrossRef](#)]
46. Dong, D.M.; Zhao, C.J.; Zheng, W.G.; Zhao, X.D.; Jiao, L.Z. Spectral characterization of nitrogen in farmland soil by laser-induced breakdown spectroscopy. *Spectr. Lett.* **2013**, *46*, 421–426. [[CrossRef](#)]
47. Harris, R.D.; Cremers, D.A.; Ebinger, M.H.; Bluhm, B.K. Determination of nitrogen in sand using laser-induced breakdown spectroscopy. *Appl. Spectrosc.* **2004**, *58*, 770–775. [[CrossRef](#)] [[PubMed](#)]
48. Wang, Q.Y.; Chen, A.M.; Qi, H.X.; Xu, W.P.; Zhang, D.; Wang, Y.; Li, S.Y.; Jiang, Y.F.; Jin, M.X. Influence of distance between sample surface and geometrical focal point on CN emission intensity from femtosecond laser-induced PMMA plasmas. *Phys. Plasmas* **2019**, *26*, 073302. [[CrossRef](#)]

**Disclaimer/Publisher's Note:** The statements, opinions and data contained in all publications are solely those of the individual author(s) and contributor(s) and not of MDPI and/or the editor(s). MDPI and/or the editor(s) disclaim responsibility for any injury to people or property resulting from any ideas, methods, instructions or products referred to in the content.